

Meta-DAN: towards an efficient prediction strategy for page-level handwritten text recognition

Denis Coquenat*

Univ Rennes, CNRS, IRISA - UMR 6074, F-35000 Rennes, France

Abstract

Recent advances in text recognition led to a paradigm shift for page-level recognition, from multi-step segmentation-based approaches to end-to-end attention-based ones. However, the naïve character-level autoregressive decoding process results in long prediction times: it requires several seconds to process a single page image on a modern GPU. We propose the Meta Document Attention Network (Meta-DAN) as a novel decoding strategy to reduce the prediction time while enabling better context modeling. It relies on two main components: windowed queries, to process several transformer queries altogether, enlarging the context modeling with the near future; and multi-token predictions, whose goal is to predict several tokens per query instead of only the next one. We evaluate the proposed approach on 10 full-page handwritten datasets and demonstrate state-of-the-art results on average in terms of character error rate. Source code and weights of trained models are available at https://github.com/FactoDeepLearning/meta_dan.

Keywords: Handwritten Text Recognition, multi-token prediction, Document Attention Network, full-page.

*Corresponding author

Email address: denis.coquenat@irisa.fr (Denis Coquenat)

1. Introduction

Handwritten Text Recognition (HTR) is the process of automatically extracting handwritten text from a digitized image and converting it into machine-readable text. The historical approach to tackle this task, still in the majority today, consists of a multi-stage paradigm. A document image is segmented into sections of text, which are then ordered to preserve a coherent reading order. Thereafter, these text sections are recognized and reassembled to obtain the overall transcription. Over time, the nature of the textual section has broadened, from the isolated character [1], to the word [2], then to the line [3, 4, 5] and more recently to the paragraph [6, 7, 8, 9], gradually increasing the context usable during recognition. However, regardless of the granularity, this multi-step approach comes with significant drawbacks: 1) the segmentation step requires an additional segmentation model and annotations, 2) the ordering step is generally a dataset-specific hand-crafted algorithm, 3) the recognition of the individual sections is carried out independently, limiting the context modeling during prediction, 4) errors accumulate in each of these steps.

More recently, the Document Attention Network (DAN) [10] was proposed as the first end-to-end approach for HTR at page level, achieving similar recognition performance compared to the multi-step approach. The DAN architecture includes a transformer-based decoder to perform a character-level autoregressive prediction process. Due to its state-of-the-art performance, the DAN is currently the default approach used for end-to-end handwritten text recognition at page-level [11, 12]. In addition, it has been extended to handle other tasks at page level such as named entity recognition [13, 14], table recognition [15], and key-value information extraction [16, 17], by adding dedicated tokens in the predictable token set.

The main drawback of the DAN, which is also an advantage, lies in its character-level iterative prediction process. Indeed, on the one hand, processing text at character level reduces the vocabulary, making training easier. It also enables to manipulate lower-dimensional latent states, since each token carries

little information, reducing computational complexity. On the other hand, it increases the target sequence length, and so the number of decoding iterations, increasing the prediction time.

In this work, we propose the Meta Document Attention Network (Meta-DAN), a novel prediction strategy to improve both inference speed and recognition accuracy for end-to-end page-level handwritten text recognition. It lies on the combined use of two distinct approaches. The first one is based on *multi-token predictions* as it showed interesting results for Natural Language Processing (NLP) [18]. The second consists of *windowed queries*, *i.e.*, processing successive transformer queries altogether as a sliding window to process them in parallel. Our main contributions are as follows:

- We propose two prediction strategies to improve page-level handwritten text recognition: windowed queries and multi-token predictions.
- We study the introduction of a confidence-based dynamic prediction policy to strike a balance between prediction speed and recognition performance for multi-token predictions.
- We provide an extensive evaluation over 10 various public datasets. To our knowledge, this is the largest benchmark evaluated at page-level. This evaluation highlights that combining both proposed approaches (Meta-DAN) leads to on-average state-of-the-art recognition performance.

2. Related Works

2.1. Handwritten text recognition

State-of-the-art approaches can be divided into two main categories we refer to as the *alignment-based* and the *attention-based* approaches.

The *alignment-based* approaches consider the recognition task as a one-dimensional sequence alignment problem between a predicted probability lattice and a ground truth sequence. The Connectionist Temporal Classification

(CTC) [19] was proposed in 2006 to perform this alignment, enabling the end-to-end recognition of word [20, 21] and line [3, 5] images.

However, the CTC only deals with one-dimensional sequences. This way, tricks have been proposed to assimilate a paragraph to a long line of text, through bilinear interpolations [8], or concatenation [22]. But, to our knowledge, alignment-based approaches are not suited for end-to-end full-page recognition, since the complexity of page layouts (*e.g.*, multi-column pages) prevent to reduce it to a one-dimensional sequence alignment problem.

More recently, the *attention-based* approaches emerged, particularly with the rise in popularity of the Transformer architecture [23]. They rely on attention mechanisms to provide an iterative autoregressive decoding process at character level, performing a kind of implicit character segmentation through the attention maps.

Contrary to the alignment-based approaches, the attention-based approaches can be applied to any input image, from a single line [4, 24] or paragraph [7, 25] to a two-page document with the DAN-based works [10, 11, 13].

It has to be noted that marginal works [6, 9] were proposed to handle paragraph recognition with a *hybrid* approach combining the attention mechanisms, to generate an implicit line segmentation, and the alignment-based approach, to recognize them iteratively through CTC decoding. In addition, an attempt to adapt the CTC to 2D-to-1D alignment was proposed in [26], but it did not lead to convincing results.

In summary, alignment-based approaches are advantageous because of their one-shot prediction, but they are limited to images with a single column of text, whereas attention-based approaches are capable of handling entire pages with complex layouts, but involve longer prediction times due to their autoregressive nature.

In this work, we focus on reducing the prediction time of the attention-based character-level approach to reach fast end-to-end page-level predictions, while improving the context modeling through the integration of the near future in the decoding process.

2.2. Speeding up autoregressive processes

The prediction time issue of autoregressive decoders is not limited to HTR. In [27], a *multi-token prediction* strategy was proposed to speed up text summarization: a transformer model is trained to predict the n future tokens at once using n projection heads. This idea was also successfully applied for neural machine translation [28] and for large language models [18].

The authors of [29] proposed another way to reduce the prediction time for the task of image captioning. The target sequence is split into subgroups of words, which are decoded in parallel.

Closer to our work, a similar approach was proposed to speed up the Document Attention Network by splitting the decoding process into two stages [11]. The first stage is dedicated to predicting the first character of each line, and the second one consists in completing all lines in parallel, reducing the number of decoding steps.

The *windowed queries* we propose also rely on the idea of processing queries in parallel, but they differ in that the processed queries are successive, leading to a unique decoding stage and a context mixing full past and near future.

An alternative to speed up the prediction process is to reduce the length of the target sequence, by relying on a dedicated tokenizer, such as the Byte-Pair Encoding (BPE) algorithm [30].

This technique was applied in [13], showing a significant prediction time decrease, in return for a higher character error rate. The approach we propose is compatible with this kind of technique as it relies on the token prediction strategy, regardless of the nature of the tokens.

In this paper, we propose to combine both windowed queries and multi-token predictions to speed up the prediction process while improving the context modeling capability of the model.

3. Background

3.1. HTR problem formulation

Given an input image \mathbf{X} , the goal is to extract the textual information \mathbf{y} in a human-coherent order. The input image $\mathbf{X} \in \mathbb{R}^{H \times W \times C}$ can be of variable size with height H , width W , and encoded over C channels (typically 1 for grayscale, and 3 for RGB). The output \mathbf{y} corresponds to the whole textual information, *i.e.*, all the text lines put together. We note \mathbf{l}^i the i^{th} text line of length L_i . The text lines \mathbf{l}^i are sequences of characters $\mathbf{l}^i = [\mathbf{l}_1^i, \dots, \mathbf{l}_{L_i}^i]$ such that $\mathbf{l}_j^i \in \mathcal{A}^c$, where \mathcal{A}^c is a given alphabet ($|\mathcal{A}^c|$ refers to its cardinality). The global output \mathbf{y} is the concatenation of the N text lines that make up the document, separated by a special join token (typically a white space or new line character). In this way, $\mathbf{y} = [\mathbf{l}_1^1, \dots, \mathbf{l}_{L_1}^1, \backslash\mathbf{n}, \mathbf{l}_1^2, \dots, \mathbf{l}_{L_2}^2, \backslash\mathbf{n}, \dots, \mathbf{l}_1^N, \dots, \mathbf{l}_{L_N}^N]$ has a length of $L^y = \sum_{i=1}^N L_i + N - 1$ and $\mathbf{y}_1 = \mathbf{l}_1^1$.

3.2. Document Attention Network

The Document Attention Network (DAN) [10] was proposed to tackle this task as a character-level autoregressive prediction process. It refers to a deep neural network illustrated in Figure 1. It is made up of two main building blocks: a Fully Convolutional Network (FCN) encoder and a causal transformer-based decoder. The general idea of this approach is as follows. Based on the image features extracted by the encoder, and on the previously predicted tokens, the goal is to predict the next token (*i.e.*, a character). To determine when to stop this iterative decoding process, a special end-of-transcription token ($\langle\mathbf{e}\rangle$) is added to the set of predictable tokens \mathcal{A} , and appended to the ground truth sequence: $\mathbf{y} \in \mathcal{A}^{L^y+1}$ with $\mathcal{A} = \mathcal{A}^c \cup \{\langle\mathbf{e}\rangle\}$ and $\mathbf{y}_{L^y+1} = \langle\mathbf{e}\rangle$.

Regarding the notations, given that matrices change over the decoding iterations, we opted for the following convention. The exponent specifies the version of the matrix at a given time, and the index specifies a vector from that matrix. For instance, in Figure 1, \mathbf{q}^t is the matrix of query token vectors at decoding iteration t made up of t vectors indexed from 0 to $t-1$. Given that the vector \mathbf{q}_i^t

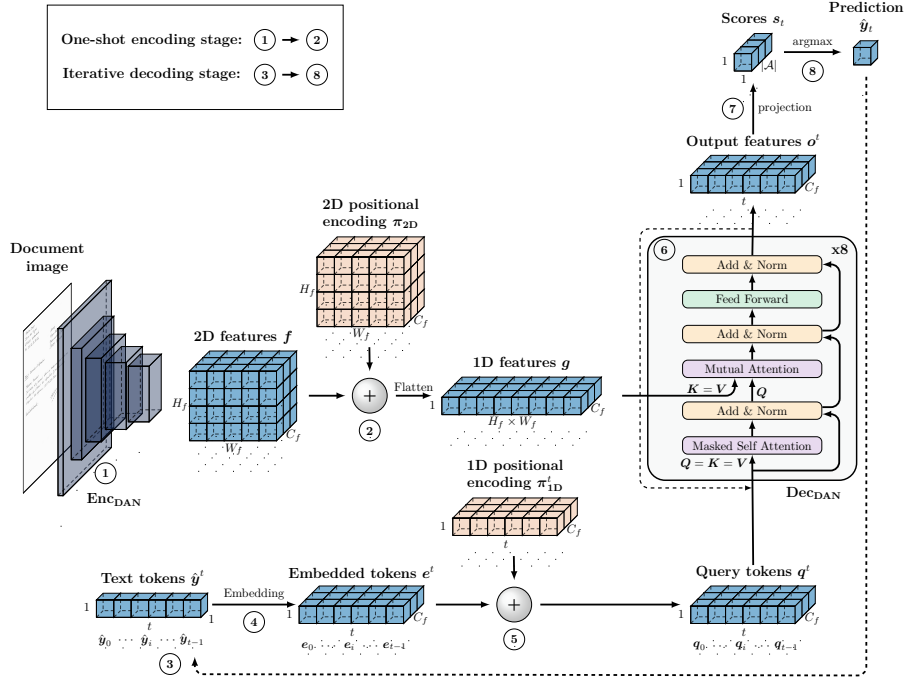


Figure 1: DAN architecture. Encoding stage: 2D features \mathbf{f} are extracted from the input image through a Fully Convolutional Network (FCN). Decoding stage: at each iteration t , a query sequence \mathbf{q}^t is generated from the previous predictions $\hat{\mathbf{y}}^t$ and associated with the image features through the transformer’s attention mechanisms to predict the next token $\hat{\mathbf{y}}_t$. The decoding is initialized with a start-of-prediction token $\hat{\mathbf{y}}_0 = \langle s \rangle$ and stops when the end-of-transcription token $\langle e \rangle$ is predicted.

at index i is the same for all t , it can be referred to as \mathbf{q}_i , omitting the exponent for readability. In the following, we describe the different stages implied by the DAN by referring to the circled numbers indicated in Figure 1.

① The DAN encoder, noted Enc_{DAN} , extracts 2D features $\mathbf{f} = \text{Enc}_{\text{DAN}}(\mathbf{X})$ ($\mathbf{f} \in \mathbb{R}^{H_f \times W_f \times C_f}$) from the input image by reducing the height by 32 and the width by 8 ($H_f = \frac{H}{32}$, $W_f = \frac{W}{8}$ and $C_f = 256$). This encoder was first proposed in [9] as a generic feature extractor for handwritten text recognition able to deal with images of variable sizes. All details can be found in the original paper [9].

② For transformer needs, positional information is injected into the image features \mathbf{f} through additive 2D positional encoding $\pi_{2\text{D}}$ [25]. Height and width

are each encoded over half of the vector channels. The result is reshaped to a one-dimensional representation: $\mathbf{g} = \text{flatten}(\mathbf{f} + \boldsymbol{\pi}_{2D})$.

③ For each iteration t , the previously predicted tokens are put together to be used by the model to know which character token should be predicted next: $\hat{\mathbf{y}}^t = [\hat{\mathbf{y}}_0, \dots, \hat{\mathbf{y}}_{t-1}]$. A special start-of-transcription token ($\langle s \rangle$) is used to initiate the prediction process: $\hat{\mathbf{y}}_0 = \langle s \rangle$.

④ A trainable weight matrix $\mathbf{E} \in \mathbb{R}^{(|\mathcal{A}|+1) \times C_f}$ is used to map each token of the vocabulary \mathcal{A} to a vector of dimension C_f , leading to $\mathbf{e}^t \in \mathbb{R}^{t \times C_f}$, with $\mathbf{e}_i^t = \mathbf{E}\hat{\mathbf{y}}_i$. One can note the additional embedding vector (+1), which corresponds to the start-of-transcription token ($\langle s \rangle$).

⑤ As the transformer attention mechanism is permutation equivariant, one-dimensional positional encoding $\boldsymbol{\pi}_{1D}^t$ [23] is added to these embeddings to preserve the order information of the tokens, resulting in the query sequence $\mathbf{q}^t = \mathbf{e}^t + \boldsymbol{\pi}_{1D}^t$.

⑥ The query tokens \mathbf{q}^t are processed through the DAN decoder, noted Dec_{DAN} , which corresponds to 8 stacked transformer decoder layers preserving the number of channels C_f . The goal is to extract relevant information from the flattened image features \mathbf{g} , *i.e.*, a latent representation \mathbf{o}_{t-1}^t of the next character to predict: $\mathbf{o}^t = \text{Dec}_{\text{DAN}}(\mathbf{q}^t, \mathbf{g})$.

⑦ Based on the last output of the decoder \mathbf{o}_{t-1} , a score vector $\mathbf{s}_t \in \mathbb{R}^{|\mathcal{A}|}$ is computed through a linear projection layer of trainable weights $\mathbf{W} \in \mathbb{R}^{|\mathcal{A}| \times C_f}$ to associate a score with each predictable token:

$$\mathbf{s}_t = \mathbf{W}\mathbf{o}_{t-1}. \quad (1)$$

⑧ The predicted token $\hat{\mathbf{y}}_t$ corresponds to the one with the highest score: $\hat{\mathbf{y}}_t = \arg \max(\mathbf{s}_t)$.

Steps ③ to ⑧ are repeated until the specific end-of-transcription token ($\langle e \rangle$) is predicted.

The DAN is trained using the cross-entropy loss \mathcal{L}_{CE} over the sequence of

logits of the scores obtained through softmax activation:

$$\mathcal{L}_{\text{DAN}} = \sum_{t=1}^{L^y+1} \mathcal{L}_{\text{CE}}(\mathbf{y}_t, \mathbf{p}_t), \quad (2)$$

where $\mathbf{p}_{t,i} = \frac{e^{\mathbf{s}_{t,i}}}{\sum_j e^{\mathbf{s}_{t,j}}}$ is the predicted probability associated with token i at time t .

3.3. Faster DAN

The Faster DAN [11] was proposed as a decoding alternative to speed up the inference stage. It aims to parallelize the text line predictions by relying on a two-stage approach. First, an autoregressive process predicts the first character of each line, following the original DAN strategy. Then, all lines are completed in parallel, reducing the total number of iterations. The main difference appears in that second decoding stage. Instead of using the output corresponding to the last token \mathbf{o}_{t-1} only, the token prediction is performed using the outputs corresponding to the last token of each text line. In this way, for N text lines, there are N token predictions per iteration. Equation 1 becomes: $\mathbf{s}_t^l = \mathbf{W}\mathbf{o}_{t-1}^l$, where \mathbf{s}_t^l is the score vector associated with the token prediction of the next character for line l at iteration t , and \mathbf{o}_{t-1}^l is the transformer output corresponding to the last predicted token for line l .

Although the Faster DAN showed interesting inference speed improvements, it results in a loss of past context when predicting a character. Indeed, instead of benefiting from the whole past context as is the case for the DAN, the Faster DAN has a partial view of the past and future due to the parallel line predictions, which reduces its ability to model the language.

The strategy we propose aims to get the best of both worlds: improving context modeling by processing successive queries altogether through multi-token predictions, while reducing prediction time through parallelization.

4. Meta Document Attention Network

We propose two new approaches for the autoregressive prediction of text tokens in the context of end-to-end handwritten text recognition at page level. For both, the idea is to predict multiple tokens at each decoding iteration to reduce the number of decoding steps, while preserving the whole past context. We assume this is a key element to reduce the number of recognition errors through language modeling. First, we propose to perform multiple predictions from the same query \mathbf{q}_{t-1} , to predict the m next tokens at once. This is referred to as the Document Attention Network with Multi-Tokens predictions (MT-DAN). Second, we propose a query approach based on a window mechanism to process multiple queries at once, each associated with a single prediction. This is referred to as the Document Attention Network with Windowed queries (W-DAN). Finally, we design a global strategy including these two approaches, called Meta Document Attention Network (Meta-DAN). A visual comparison of the prediction processes is depicted in Figure 2.

4.1. MT-DAN

Inspired by recent works on multi-token predictions for Natural Language Processing (NLP) [18], we propose the Document Attention Network with Multi-Tokens predictions (MT-DAN). It relies on the following process. Based on the last query output \mathbf{o}_{t-1} , m projection heads are used to compute the scores for the m next tokens, with m being a new hyperparameter. Equation 1 becomes:

$$\mathbf{s}_{t+k}^{(t-1)} = \mathbf{W}^k \mathbf{o}_{t-1}, \quad (3)$$

where $\mathbf{s}_{t+k}^{(t-1)}$ is the score vector associated with the token prediction of the k^{th} next token computed at iteration t . The exponent $(t-1)$ indicates that this prediction was performed based on query indexed by $t-1$. \mathbf{W}^k is the weight matrix corresponding to the k^{th} projection head, and \mathbf{o}_{t-1} is the transformer output corresponding to the last query token \mathbf{q}_{t-1} . In this way, m predictions are performed per iteration following:

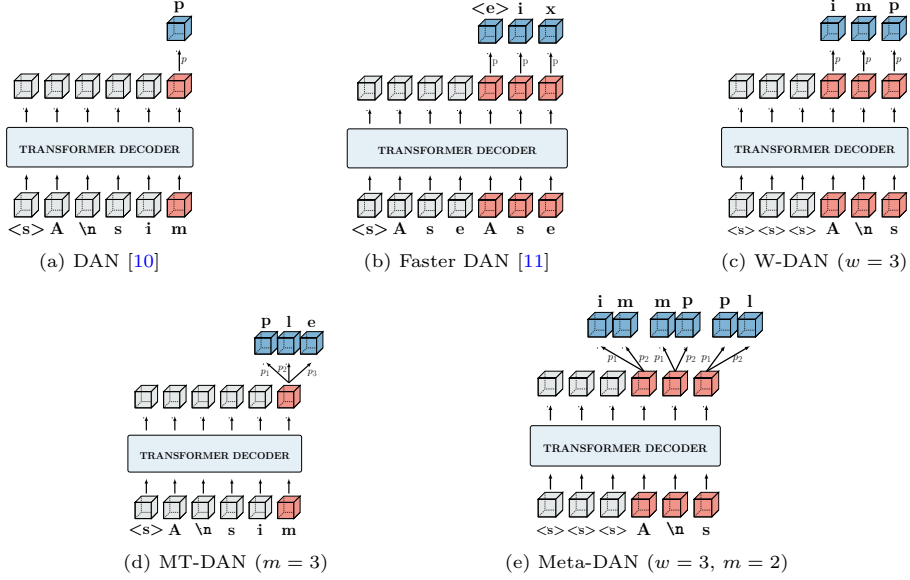


Figure 2: Comparison of the prediction strategies for the target sequence "A\nsimple\nexample.", under three aspects: 1) the number of predictions per query (single for DAN, Faster DAN and W-DAN); 2) the number of queries processed at once per decoding iteration (single for DAN and MT-DAN); 3) the available context (start of each line for Faster DAN; full past for the others). The Meta-DAN groups together the advantages of each of these points: it processes multiple queries at once, each one leading to several token predictions, and benefits from the full past context.

$$\hat{\mathbf{y}}_{t+k}^{(t)} = \arg \max(\mathbf{s}_{t+k}^{(t)}), \quad (4)$$

with $k \in [0, \dots, m - 1]$.

As one can note, several predictions $\hat{\mathbf{y}}_{t+k}^{(t)}$ are associated with the same target token \mathbf{y}_{t+k} . This is not an issue during training; we train the MT-DAN using the cross-entropy loss over the whole token sequence, as for the original DAN. It involves adding $m - 1$ extra $\langle e \rangle$ tokens in order for all text tokens to have a target for each of the projection heads, leading to the following loss:

$$\mathcal{L}_{\text{MT-DAN}} = \sum_{t=1}^{L^y+1} \sum_{k=0}^{m-1} \mathcal{L}_{\text{CE}}(\mathbf{y}_{t+k}, \mathbf{p}_{t+k}^{(t)}), \quad (5)$$

with $\mathbf{p}_{t+k}^{(t)} = \text{soft max}(\mathbf{s}_{t+k}^{(t)})$.

Predicting multiple tokens $\hat{\mathbf{y}}_{t+k}$ from a unique output \mathbf{o}_{t-1} can theoretically

lead to saturation as m increases. Indeed, the fixed-size vector \mathbf{o}_{t-1} must represent the next m text tokens at once. To solve this issue, we propose another way to predict multiple tokens per iteration, which consists in processing several consecutive queries at once.

4.2. W-DAN

To solve the MT-DAN output compression issue, we propose the Document Attention Network with Windowed queries (W-DAN). Instead of relying on a single output to predict m tokens, we opt for using the output of the last w predictions to predict the w next tokens, w being a new hyperparameter. In this way, it solves the compression issue as there are as many outputs as there are predictions. The decoding process of the W-DAN acts as a sliding window over the query tokens, processing them by chunks of w tokens at once, leading to w new outputs. More precisely, each output \mathbf{o}_{t-q} is responsible for the prediction of a single token $\hat{\mathbf{y}}_{t-q+w}$, with $q \in [1, \dots, w]$. Equation 1 becomes:

$$\mathbf{s}_{t-q+w} = \mathbf{W}\mathbf{o}_{t-q}, \quad (6)$$

with

$$\hat{\mathbf{y}}_{t-q+w} = \arg \max(\mathbf{s}_{t-q+w}). \quad (7)$$

It has to be noted that all scores \mathbf{s}_{t-q+w} are computed using the same projection head of weights \mathbf{W} as they are applied independently on each \mathbf{o}_{t-q} . In addition, it is necessary to initialize the decoding process with w initial tokens to predict the first w tokens. We arbitrarily choose to use the same start-of-transcription token w times ($\hat{\mathbf{y}}_0 = \dots = \hat{\mathbf{y}}_{w-1} = \langle s \rangle$). We also added n_e extra end-of-transcription tokens at the end of the target sequence so as to make the target length divisible by w . It leads to the following loss:

$$\mathcal{L}_{\text{W-DAN}} = \sum_{t=w}^{L^y+1+n_e} \mathcal{L}_{\text{CE}}(\mathbf{y}_t, \mathbf{p}_t). \quad (8)$$

The major advantage of both presented approaches compared to the DAN

and the Faster DAN is that the k or w predictions are consecutive and performed altogether: the context is enlarged when the prediction takes place. The model must focus on a broader context to predict multiple successive tokens. For instance, for $k = 3$ (or $w = 3$), the model focuses on predicting $\{\hat{\mathbf{y}}_t, \hat{\mathbf{y}}_{t+1}, \hat{\mathbf{y}}_{t+2}\}$ at once. This way, the prediction of $\hat{\mathbf{y}}_t$ is impacted by the future context $\{\hat{\mathbf{y}}_{t+1}, \hat{\mathbf{y}}_{t+2}\}$, which improves the ability to model the language at prediction time compared to DAN.

4.3. Meta-DAN

We propose to take advantage of both presented approaches by combining them: this is referred to as the Meta Document Attention Network (Meta-DAN). Thus, the Meta-DAN is parametrized by two hyperparameters m and w , indicating the number of projection heads and the window size, respectively. In other words, at each iteration t , a window of w query tokens $\{\mathbf{q}_{t-w}, \dots, \mathbf{q}_{t-1}\}$ are processed at once, each one leading to m predictions. More precisely, the output of the query token \mathbf{q}_{t-q} , *i.e.* \mathbf{o}_{t-q} , is responsible for the prediction of $\{\hat{\mathbf{y}}_{t-q+w}, \dots, \hat{\mathbf{y}}_{t-q+w+m-1}\}$ as follows:

$$\hat{\mathbf{y}}_{t-q+w+k}^{(t-q)} = \arg \max(\mathbf{s}_{t-q+w+k}^{(t-q)}), \quad (9)$$

with

$$\mathbf{s}_{t-q+w+k}^{(t-q)} = \mathbf{W}^k \mathbf{o}_{t-q}, \quad (10)$$

where $\mathbf{s}_{t-q+w+k}^{(t-q)}$ is the score associated with token $\hat{\mathbf{y}}_{t-q+w+k}$ by the k^{th} projection head of the q^{th} query token in the query window, and with $k \in [0, \dots, m-1]$ and $q \in [1, \dots, w]$. The Meta-DAN involves initializing the decoding process with w $\langle s \rangle$ tokens, as for the W-DAN, and adding n_e extra $\langle e \rangle$ so that the last query has a target prediction for all its associated projection heads. Regarding training, equation 2 becomes:

$$\mathcal{L}_{\text{Meta-DAN}} = \sum_{t=w}^{L^y+1+n_e} \sum_{k=0}^{m-1} \mathcal{L}_{\text{CE}}(\mathbf{y}_{t+k}, \mathbf{p}_{t+k}^{(t)}) \quad (11)$$

As one can note, several query tokens can be in charge of the same prediction. This is shown in Figure 2e with an example with $w = 3$ and $m = 2$: the "m" and "p" are predicted twice, from two different queries. In this work, we limit ourselves to using the prediction of the first projection head for the $w - 1$ first queries, and the prediction of all projection heads for the last one. Although discarded, we assume that training to predict these extra characters encourages the network to improve language modeling.

In summary, the Meta-DAN is a general formulation for which one can distinguish three specific cases depending on the hyperparameters:

- Choosing $m = 1$ and $w = 1$ consists in the DAN approach.
- Choosing $m > 1$ and $w = 1$ results in the MT-DAN approach.
- Choosing $m = 1$ and $w > 1$ leads to the W-DAN approach.

4.4. Impact on the computational complexity

To further give insights into the main differences between all these prediction strategies, Figure 3 provide visuals of the attending maps (transformer masks), stating which token can access to which other tokens for the masked self-attention.

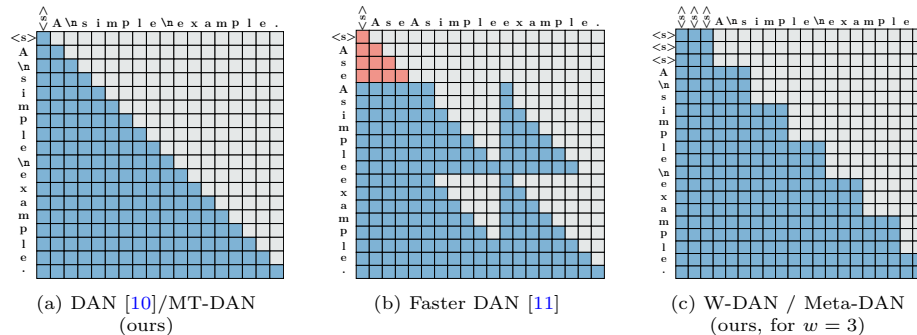


Figure 3: Comparison of attention context for the target sequence "A\nsimple\nexample.". The blue color indicates which tokens can be attended (column) when processing a given token (line). Grey cells corresponds to ignored tokens (*i.e.*, not yet predicted tokens). Red color highlights the first pass of the Faster DAN.

Regarding the MT-DAN approach, the attending maps of the DAN and the MT-DAN are identical, no matter the value of m ; this means that they both imply the same computations in the transformer decoder layers. In addition, contrary to the NLP application, which relies on the Byte-Pair Encoding algorithm leading to large vocabularies, the addition of extra projection heads does not significantly impact the global computational complexity as we are working at character level, limiting the dimensions of the projection weight matrices.

Concerning the W-DAN approach (and thus the Meta-DAN), the attending maps show that there are more interactions between the tokens in the self-attention layers, resulting in more computations, theoretically. However, to our knowledge, the current implementations of the transformer rely on masks to "hide" the forbidden tokens (usually the future) *after* the query-key multiplication takes place. In this way, this does not impact the computation time in practice since computations are performed over all token pairs, whether they are really used or not.

No matter the approach, the prediction process can be parallelized at training time using teacher forcing [31], *i.e.*, by injecting the whole ground truth instead of the autoregressive previous predictions, so that all decoding iterations are performed at once. In this way, there is no extra benefit for the training stage. The major impact is positive and related to the time complexity at prediction time when parallelizing the computation of token predictions.

5. Experimental conditions

5.1. Datasets

We select 10 public datasets with high diversity to make our evaluation robust: IAM [32], READ-2016 [33], Esposalles [34], BRESSAY [35], Scribble-Lens [36], Esparchos [37], CASIA-2 [38], MAURDOR [39], RIMES-2009 [40] and RIMES-2024 [41]. As detailed in Table 1, they cover 8 languages, three alphabets (Latin, Greek, and Chinese), and 6 centuries. They also involve many

writing configurations (from a single writer to more than a thousand), various sizes of character sets, as well as a variable amount of training data.

Table 1: Detailed features of evaluated datasets (page-level).

Dataset	Train	Val	Test	Charset size	Average # char/page	Language	Century	Writers
IAM (paragraph) [32]	747	161	336	80	371	English	20 th -21 st	657
RIMES-2009 [40]	1,050	100	100	108	588	French	21 st	≈ 400
RIMES-2024 [41]	4,500	505	600	123	567	French	21 st	≈ 1,400
READ-2016 [33]	350	50	50	89	468	German	15 th -19 th	unknown
Esposalles [34]	75	25	25	62	1,748	Catalan	17 th	1
BRESSAY [35]	647	154	199	109	2,612	Portuguese	21 st	1,000
ScribbleLens [36]	164	14	21	85	1,410	Dutch	16 th -18 th	85
Eparchos [37]	80	20	20	157	962	Greek	16 th	2
CASIA-2 [38]	3,600	475	1,015	2,704	273	Chinese	21 st	1,019
MAURDOR-C3 [39]	1,006	148	166	134	491	French/English	21 st	> 130
MAURDOR-C4 [39]	721	111	114	127	675	French/English	21 st	> 90

We used the standard split into training, validation, and test sets when existing. To our knowledge, we are the first to use the recently released RIMES-2024 dataset, so we propose a split, randomly sampling for training, validation and test by respecting the split provided at line level in 2011 [42]. We discarded images from the "Q" category, which corresponds to forms, since they do not provide the whole transcript. For ScribbleLens, we removed 10% of the training samples to create a validation set by randomly picking from each of its data sources. For Eparchos, we propose a split at page level, by taking 80% of the samples for training, 10% for validation, and 10% for test. Appendix A provides the splits at line level, used for pre-training purposes, for the datasets providing line-level annotations. This section also includes document image examples.

5.2. Training strategy

If not stated otherwise, we follow the main guidelines described in [10]:

- The encoder is pre-trained using a CTC-based line-level training strategy. An adaptive max-pooling layer is added on top of the encoder to collapse the vertical axis, leading to a one-dimensional sequence of features. Then, a classification layer is applied to generate a probability lattice. If line-level annotations are provided in the dataset, we use a ratio of 25% real / 75% synthetic images (100% synthetic otherwise).

- Data augmentation is applied with a probability of 90%, including resolution change, color jittering, Gaussian noising, Gaussian blurring, elastic distortion, dilation, erosion, and perspective transformation.
- The page-level training relies on a curriculum synthetic document generation strategy. The generated images contain more and more text lines through training. The ratio of synthetic documents slowly decreases from 90% to 10%. Following [13], we rely on the 1001-fonts.com website to get a large collection of fonts from which we randomly sample when rendering a synthetic text line. The text used for synthetic generation is from the training set of the target dataset.
- Line-level pre-training is carried out using 5M training samples; page-level training (including curriculum) is performed over 1M samples. Training and pre-training are performed using the Adam optimizer with an initial learning rate of 10^{-4} , and automatic mixed-precision.
- Preprocessing: images are scaled to reach 150 dpi resolution. No post-processing: we do not use any external data or language model.

5.3. Evaluation

We compute the standard Character Error Rate (CER) and Word Error Rate (WER) to evaluate the text recognition performance. Both metrics are computed using the Levenshtein distance [43], which counts the number of deletion, addition, and substitution operations required to go from the prediction sequence to the ground truth sequence, normalized by the length of the ground truth sequence. While the CER considers the prediction and the ground truth as sequences of characters, the WER considers them as sequences of words. All results are given for the test sets. It has to be noted that page-level approaches are sensitive to reading order; it means that correct text recognized in a wrong order will be considered as incorrect. For each model, we compute the average prediction time for one test image when using a single A100 GPU and a mini-batch size of 1. We set the maximum number of decoding iterations for

all datasets to 5,000 to cover the requirements of all evaluated datasets. This way, we do not rely on dataset-specific properties, which is closer to a real-case scenario. It has to be noted that this choice results in recognition metrics that can be highly impacted by the prediction loops that can occur, *i.e.*, when the model predicts again and again the same text line.

6. Experiments

In this section, we evaluate the proposed approaches (W-DAN, MT-DAN, and Meta-DAN) on the IAM and BRESSAY datasets to select the best approach and hyperparameters. Then, we apply them to the other 9 datasets to validate the robustness of the approach. While relying on the original DAN architecture [10], we propose an enlarged version of the encoder, which we refer to as FCN-M as it shows better recognition performance (details in [Appendix B](#)).

6.1. W-DAN

Table 2(a) provides the results of the W-DAN approach for several window sizes w . It highlights that it is possible to predict up to 10 character tokens at once, while being competitive in terms of CER. It is especially true for the BRESSAY dataset for which $w = 10$ leads to a small increase of only 0.23 points of CER. However, results degrade significantly for $w = 25$ with a CER of 6.56% instead of 4.23% for IAM, and 4.37% instead of 2.43% for BRESSAY.

As one can note, it is possible to reduce the average prediction time per sample nearly linearly with respect to the window size. Regarding BRESSAY prediction times, it appears that the new implementation has impacted the prediction time for large text predictions, leading to a lag in the speed factor improvement. A main observation is that the model is harder to train as w increases. We assume that this is due to the inherent complexity of the self-attention layer, which grows with the length of the query sequence. Indeed, the more query tokens are processed altogether, the greater the required effort to coordinate and focus on the right parts of the image features. In this way, we

needed to increase the amount of training data to reach convergence for $w = 10$ and $w = 25$ up to 2M and 3M, respectively.

Table 2: Comparison of W-DAN and MT-DAN performance with respect to the window size w and to the number of token heads m , respectively, on the IAM and BRESSAY test sets.

(a) W-DAN results.					(b) MT-DAN results.				
w	IAM		BRESSAY		m	IAM		BRESSAY	
	CER (%)	Time (s)	CER (%)	Time (s)		CER (%)	Time (s)	CER (%)	Time (s)
1 (DAN)	4.23	3.39	2.43	24.65	1 (DAN)	4.23	3.39	2.43	24.65
2	4.67	1.94	2.91	20.86	2	4.70	1.84	2.47	13.02
3	4.83	1.26	3.05	12.25	3	4.74	1.23	2.46	8.85
4	4.75	0.97	2.63	8.63	4	4.68	0.93	2.70	6.64
5	4.87	0.77	3.02	6.63	5	5.14	0.75	2.45	5.28
10*	5.07	0.40	2.66	2.95	10*	5.06	0.39	2.37	2.64
25*	6.56	0.18	4.37	1.13	25*	7.19	0.16	3.15	1.11

* More training data was used for $w = 10$, $m = 10$, $w = 25$, and $m = 25$

6.2. MT-DAN

For fair comparison, we evaluate the MT-DAN approach for the same values of token heads $m \in \{1, 2, 3, 4, 5, 10, 25\}$, as both m for MT-DAN and w for W-DAN refer to the number of predicted tokens per decoding iteration. Here, $m = 1$ corresponds to the original DAN. The obtained results shown in Table 2(b) are quite similar to those of the W-DAN, with comparable recognition performance and prediction time. Neither approach seems to stand out from the other. Even for the extreme case of $m = 25$, it appears that the MT-DAN performs better for the BRESSAY dataset with a CER of 3.15% compared to 4.37% for the W-DAN (with $w = 25$), but it is the contrary for the IAM dataset: 7.19% of CER compared to 6.56% for the W-DAN. As for the W-DAN, it required more training data for $m = 10$ and $m = 25$ to reach convergence. However, this is not for the same reason. We assume that, for the MT-DAN, this is due to the compression task that is harder as m increases. Indeed, m character representations must be compressed into a single fixed-size vector. We also relied on a curriculum strategy at character level before the line-level curriculum strategy. We did not use it for the W-DAN as it was not effective; we assume this is due to the way the tokens interact to make their predictions in this approach.

Improving the prediction policy. To enhance the capacity of the MT-DAN approach, we propose and evaluate two variants, we called prediction policies, at

inference time:

- 1) The *static* prediction policy consists in always predicting the k next tokens at each decoding iteration ($k \leq m$). Previous results, shown in Table 2(b), relied on this naïve prediction policy, setting $k = m$.
- 2) The *dynamic* prediction policy involves predicting between 1 and m tokens at once, based on a confidence threshold τ . The number of predicted tokens must vary from one decoding iteration to another. The idea is to predict fewer tokens when the model is unsure of its prediction, by assuming that it could be better at the next decoding iteration, for which it will benefit from more context. The first token head is always used to avoid an infinite loop; the other $m - 1$ heads are then considered sequentially. If the confidence score (*i.e.*, the maximum value after softmax operation) associated with the current head is greater than or equal to τ , then the prediction is preserved, and the next head is processed; the decoding iteration ends otherwise.

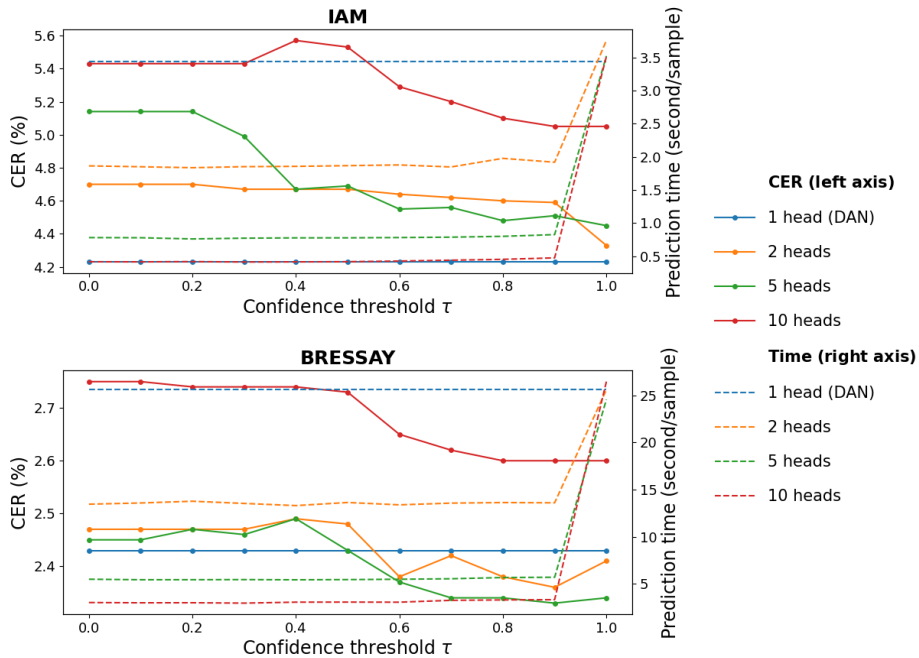


Figure 4: Accuracy-speed trade-off with respect to confidence threshold τ for dynamic decoding of the MT-DAN on IAM and BRESSAY.

We first study the choice of the confidence threshold τ for the dynamic strategy. Figure 4 shows the evolution of the CER and of the prediction time with respect to τ for values between 0 and 1, with a step of 0.1. A confidence threshold of $\tau = 0$ means that the token predicted by each projection head is always kept (the fastest option): it corresponds to the static prediction policy. A confidence threshold of $\tau = 1$ means that only the prediction of the first projection head is kept (the longest option): it results in the DAN prediction strategy. We compare the accuracy-speed trade-off for different numbers of heads on both IAM and BRESSAY datasets. We also show results for a single projection head as a baseline, leading to a CER plateau as the dynamic strategy is designed for multi-token predictions.

It appears that the confidence threshold fulfills its purpose, as there is a trend toward a decrease in the CER as τ increases, for both datasets. In addition, the prediction time per sample is rather stable from $\tau = 0$ to $\tau = 0.9$. However, one can note a huge prediction time gap going from $\tau = 0.9$ up to $\tau = 1$, making the approach ineffective as it consists in single-token prediction, as the DAN. In this way, we consider $\tau = 0.9$ as a good compromise over all the evaluated configurations and use it for the next experiments.

We compare the two prediction policies, namely static and dynamic, in Table 3. For the static prediction policy, we evaluate the models for $k \in \{1, 2, 3, 4, 5\}$ when possible. Regarding the IAM dataset, one can observe a trend whereby the CER decreases as k also decreases, with optimum performance reached for $k = 1$, noting that decreasing k highly increases the prediction time. This trend is less noticeable on the BRESSAY dataset with more fluctuating results. However, the proposed dynamic prediction policy with $\tau = 0.9$ shows interesting results, which generally outperform the corresponding model using the static strategy with $k = m$, with a limited prediction time overhead. For instance, it enables to reduce the CER from 5.14% to 4.51% for the IAM dataset ($m = 5$), while slightly increasing the prediction time from 0.75 seconds (Table 2(b)) to 0.83 seconds.

Table 3: Comparison of static and dynamic prediction policies of the MT-DAN. CER (%) are given for IAM and BRESSAY datasets. Best results are shown in bold; results that are very close to the best (whose difference in values is less than 0.05%) are underlined.

Number of heads (m)	IAM							BRESSAY						
	static					dynamic		static					dynamic	
	$k=1$	$k=2$	$k=3$	$k=4$	$k=5$	$\tau=0.9$	Time	$k=1$	$k=2$	$k=3$	$k=4$	$k=5$	$\tau=0.9$	Time
1 (DAN)	4.23	X	X	X	X	X	X	2.43	X	X	X	X	X	X
2	4.33	4.70	X	X	X	4.59	1.92	<u>2.41</u>	2.47	X	X	X	2.36	13.60
3	4.31	4.85	4.74	X	X	4.31	1.32	2.46	2.46	2.46	X	X	2.69	9.21
4	4.48	4.54	4.68	4.68	X	<u>4.52</u>	1.00	2.71	2.86	2.61	2.70	X	2.71	6.97
5	4.45	4.74	4.54	4.86	5.14	4.51	0.83	<u>2.34</u>	2.40	<u>2.36</u>	2.40	2.45	2.33	5.70
10	4.79	<u>4.80</u>	4.87	4.87	4.90	<u>4.80</u>	0.47	2.67	2.24	2.70	2.28	2.29	2.66	3.15
25	5.73	5.61	5.58	5.64	5.68	5.47	0.36	3.35	3.30	2.92	<u>2.91</u>	2.93	2.87	1.88

6.3. Meta-DAN

In this section, we focus on $m = 5$ and $w = 5$ as it seems to be a good compromise between prediction time and recognition performance. Through experiments, we found out that transfer learning from MT-DAN to Meta-DAN leads to better results than from W-DAN or line-level pre-training on both IAM and BRESSAY datasets, so we keep this setting in the following.

Comparison with MT-DAN and W-DAN. We compare the Meta-DAN with the MT-DAN and the W-DAN for the same hyperparameters ($m = 5$ and $w = 5$) in Table 4. However, it should be noted that this is not a constraint of the proposition, and that m and w can be chosen completely independently for the Meta-DAN. As one can note for the IAM and BRESSAY datasets, combining both windowed queries and multi-token predictions enable to increase the recognition performance, as well as reducing the prediction time. Compared to DAN, the conclusion is not as clear-cut regarding the character error rate as it is in favor of the DAN for IAM with a CER of 4.23% compared to 4.79%, but in favor of the Meta-DAN for BRESSAY with a CER of 2.38% compared to 2.43%. It shows that the Meta-DAN can be both more efficient and faster than the DAN, depending on the target dataset.

Comparing prediction strategies. As the Meta-DAN relies on multi-token predictions, we can apply the same dynamic prediction policy as for the MT-DAN. This is evaluated in Table 5. It appears that the confidence scores associated with the predictions are not as high as those for the MT-DAN, leading to a

Table 4: Comparison of proposed approaches using the static prediction policy ($m = k$).

Approach	m	w	IAM		BRESSAY	
			CER	Time	CER	Time
DAN	1	1	4.23	3.39	2.43	24.65
W-DAN	1	5	4.87	0.77	3.02	6.63
MT-DAN	5	1	5.14	0.75	2.45	5.28
Meta-DAN	5	5	4.79	0.43	2.38	4.01

Table 5: Comparison of Meta-DAN ($w = 5, m = 5$) performance with respect to the decoding strategy.

Strategy for concurrent	IAM		BRESSAY	
	CER	Time	CER	Time
static ($k = 1$)	4.55	0.79	2.31	7.16
static ($k = 5$)	4.79	0.43	2.38	4.01
dynamic ($\tau = 0.9$)	4.73	0.45	2.37	7.14

failure case for the BRESSAY dataset for which the prediction time is close to that of W-DAN (static case with $k = 1$). As previously, the static policy with $k = 1$ leads to the best recognition performance but suffers from longer prediction. We consider the static policy with $k = m = 5$ as the best alternative for the Meta-DAN and use this configuration in the following.

6.4. Visualization

A visualization of the attention process for the different approaches is provided in Figure 5. Images are cropped to a single line for visibility, but predictions are performed on the full-page images. Attention weights of the last cross-attention layer are projected on the input image (values are normalized such that the maximum intensity is reached for 0.2). One color is associated with each projection head in this order: red, blue, green, yellow, and cyan. As expected, the attention weights are peakier for DAN and W-DAN since each query only focuses on a single character prediction, contrary to MT-DAN and Meta-DAN that involve a multi-token prediction strategy. Interestingly, the attention weights of the MT-DAN even spread over the last predicted characters ("he ") without disturbing the recognition. The combination of multi-token predictions and window queries enables the Meta-DAN to efficiently predict more tokens (9 here) by taking advantage of more context.

6.5. Large-scale comparison of the prediction approaches

We now provide a large evaluation at page level over all datasets and prediction approaches (ours and concurrent ones). We used the same architecture and training strategy for all the evaluated settings, *i.e.*, we also train the concurrent approaches with the same k framework for fair comparisons. We also

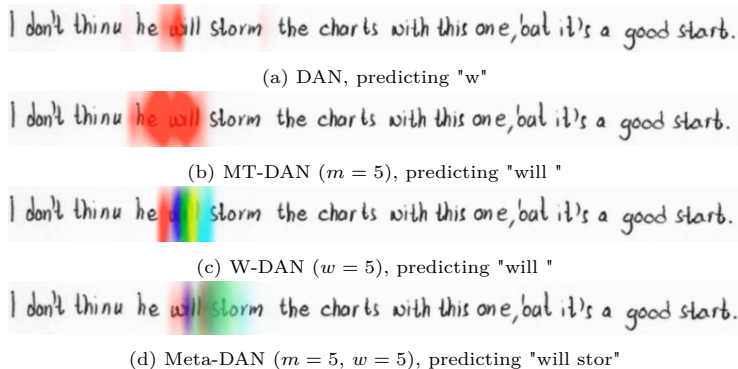


Figure 5: Visualization of the attention process for a single decoding step. Attention weights are more diffused when relying on multi-token predictions (MT-DAN, Meta-DAN)

Table 6: CER results (in percentages) on the test sets with FCN-M encoder. We used $m = 5$ and $w = 5$ for the proposed approaches. Best results at page level are in bold.

Dataset	Line-level		Page-level									
	FCN		DAN		Faster DAN		W-DAN		MT-DAN		Meta-DAN	
	CER	Time	CER	Time	CER	Time	CER	Time	CER	Time	CER	Time
IAM	4.84	0.03	4.23	3.39	4.16	0.64	4.87	0.77	4.51	0.83	4.79	0.43
BRESSAY	3.45	0.02	2.43	24.65	2.34	1.51	3.02	6.63	2.33	5.70	2.38	4.01
READ-2016	4.61	0.03	3.85	4.88	4.34	0.73	4.34	1.09	3.80	0.80	4.22	0.63
Esposalles	0.61	0.05	5.86	19.99	1.91	2.23	5.95	4.91	2.16	3.37	2.13	2.86
ScribbleLens	4.72	0.06	4.38	16.24	4.81	2.17	5.06	4.04	4.16	2.71	4.31	2.24
CASIA-2	2.91	0.05	1.10	2.81	3.17	0.57	2.81	0.69	1.32	0.52	2.01	0.43
Eparchos	7.79	0.04	7.27	9.14	7.52	0.97	8.18	2.11	8.14	1.52	7.36	1.21
RIMES-2009	x	x	6.73	5.87	6.56	0.98	6.26	1.44	4.94	1.09	4.64	0.83
RIMES-2024	x	x	3.89	5.89	3.57	0.94	3.48	1.38	2.97	1.06	3.26	0.80
MAURDOR-C3	x	x	10.38	5.34	9.76	0.78	8.05	1.27	13.71	1.16	7.93	0.69
MAURDOR-C4	x	x	8.28	6.70	10.46	1.32	6.93	1.61	6.62	1.20	6.59	0.92
Average	x	x	5.31	9.54	5.33	1.17	5.36	2.36	4.97	1.81	4.51	1.37
# parameters	17.7 M		23.1 M		23.1 M		23.1 M		23.4 M		23.4 M	

provide results at line level, which corresponds to the pre-training stage (same encoder with CTC decoding) for comparison. However, let us recall that line-level metrics only correspond to recognition on humanly-segmented images: it does not include the required segmentation and ordering stages that would lead to higher CER and prediction times. Results shown in Table 6 highlight that it is generally beneficial to process documents at page level rather than line level. A counter-example is the Esposalles dataset, where line recognition performs very well, demonstrating a certain ease of visual reading (single writer). In this particular case, it seems that the benefits of implicit language modeling provided by the transformer decoder are not sufficient to compensate for the added

difficulty of learning the reading order.

Focusing on the prediction time, all proposed approaches are on par with the prediction speed of the Faster DAN. However, one can note that the Faster DAN speed improvement is highly dependent on the number of lines to be predicted in the document, contrary to the proposed approaches. *E.g.*, the Faster DAN is 16.3 times faster than the DAN for the BRESSAY dataset (≈ 30 lines/doc) but 4.9 times faster for the CASIA-2 dataset (≈ 10 lines/doc).

Regarding the CER, the MT-DAN reaches state-of-the-art performance on 4 datasets. Also, it seems that the enlarged context provided by the Meta-DAN stabilizes the attention process, reducing the looping phenomenon (when the same text is predicted multiple times) for heterogeneous layouts as in the MAURDOR datasets. It results in new state-of-the-art recognition performance when averaging on all datasets with an improvement of 0.46 points compared to MT-DAN and 0.80 points compared to DAN. Associated WER results are given in [Appendix C](#) for completeness.

6.6. Comparison with the state of the art

We further compare the proposed approaches to the state of the art in [Table 7](#). For fair comparison, we only compare to works following the same constraints, *i.e.*, without an external language model and that do not perform training on additional external datasets. Among the 7 datasets for which there is a page-level evaluation in the literature, we reach new state-of-the-art CER on 4 of these datasets with the MT-DAN or the Meta-DAN. The proposed approaches also outperform state-of-the-art line-level recognition models on ScribbleLens and CASIA-2 datasets. One can note an exception with the Eparchos dataset, which follows a similar behavior compared to the Esposalles dataset, *i.e.*, text recognition is better at line level than at page level. This can be explained by the very few available training data that prevents from fully benefiting from the potential of attention-based models.

Table 7: Comparison with state-of-the-art approaches (no external data, no external language model). Best result at page level is shown in bold. State-of-the-art line-level results are given for comparison.

Dataset	Approaches of the literature			CER (%) for our page-level approaches	
	Architecture	Level	CER (%)	MT-DAN	Meta-DAN
BRESSAY	[35] CRNN + attention	line	3.62	2.33	2.38
	[35] YOLO-v5 + Calamari	line	6.01		
	[35] DANIEL	page	3.55		
CASIA-2	[44] CNN + attention	line	2.34	1.32	2.01
	[45] DenseNet + attention	line	1.78		
Eparchos	[37] CNN + GRU	line	4.53	8.14	7.36
Esposalles	[17] DAN + NER	line	0.48	2.16	2.13
	[17] DAN + NER	page	3.61		
IAM	[46] transformer	line	3.99	4.51	4.79
	[10] DAN	page	4.54		
	[13] DANIEL	page	4.38		
MAURDOR-C3	[10] DAN	page	8.62	13.71	7.93
	[11] Faster DAN	page	8.93		
MAURDOR-C4	[10] DAN	page	8.02	6.62	6.59
	[11] Faster DAN	page	9.88		
READ-2016	[9] VAN	line	4.10	3.80	4.22
	[10] DAN	page	3.43		
	[11] Faster DAN	page	3.95		
	[13] DANIEL	page	4.03		
RIMES-2009	[10] DAN	page	4.54	4.94	4.64
	[11] Faster DAN	page	6.38		
	[13] DANIEL	page	5.80		
RIMES-2024	X	X	X	2.97	3.26
ScribbleLens	[47] CNN + BLSTM	line	6.47	4.16	4.31

6.7. Error analysis

In this section, we propose a qualitative analysis of the errors made by the Meta-DAN. To this end, some examples of predictions and associated ground truths are shown in Figure 6 to illustrate the different kinds of errors that can occur.

The most common error is linked to visual ambiguities. For instance, the Meta-DAN predicted an "m" instead of "rr" for the word "arrived" (Figure 6b) or and "n" instead of an "r" in the word "garida" (Figure 6c). This shows that, although the proposed contributions improve context modeling, it remains limited: the model sometimes tends to rely more on visual characteristics than on linguistic context. We assume that this is due to the lack of training data in the datasets that prevents the model from really "understand" the text it predicts, leading to the prediction of "dest" instead of "de St" (Figure 6c), due

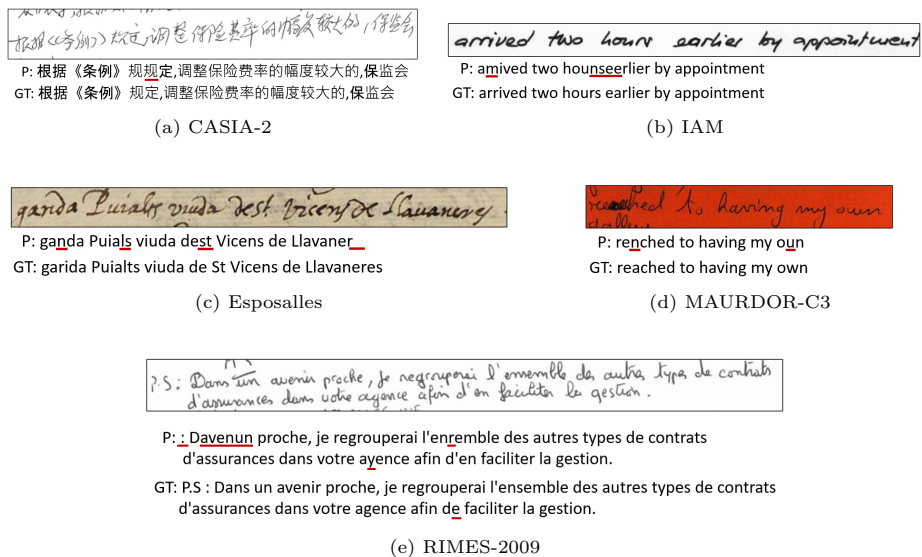


Figure 6: Visualization of errors made by Meta-DAN on test samples of various datasets. For visibility, page images were cropped and associated with Ground Truth (GT) and Prediction (P). Errors are underlined in red.

to the spacing between those two words that is not clearly visible in the image. In other words, it suffers from a lack of linguistic knowledge, but it also lacks knowledge of the world around us to clear up certain ambiguities.

Another kind of error comes from the attention-based prediction process itself. In this way, the same character might be predicted twice (Figure 6a), or some characters are missed, as in Figure 6e ("P.S"), generally due to specific layouts not seen during training. In rare cases, some characters may have been predicted in the wrong order and partially missed, as "Davenun" predicted instead of "Dans un avenir" (Figure 6e). As mentioned previously, another failure case due to the attention mechanism is related to loops, when the model predicts the same part of text, generally a whole text line, multiple times.

Although rare, predictions may be considered false, wrongly, when the ground truth contains errors as in Figure 6e: the Meta-DAN predicted "d'en", as visible in the input image, but the ground truth is "de".

7. Discussion

Through this extensive study on prediction strategies, we showed the robustness of the proposed Meta-DAN on many HTR dataset configurations, reaching on-average state-of-the-art results. However, one can note that there is no one strategy that is better on all datasets. We noticed that, no matter the prediction variant, it seems to have a beneficial impact on the loop effects, noticeable through the CER results of the Esposalles dataset (Table 6). We assume that for the Faster DAN, this is due to the parallelization of the line recognition, since loops mainly occur when switching from one line to another. For the proposed approaches, this must be the result of the increased context modeling and the forced anticipation of the model to predict the following characters, which can be found on two consecutive lines. But contrary to the Faster DAN, the Meta-DAN does not suffer from "catastrophic" errors. Indeed, any missed or duplicated character in the first decoding stage of the Faster DAN leads to discarding or duplicating a whole text line. While rare, this can severely impact the recognition performance.

Regarding the prediction time, it has to be noted that the Meta-DAN, while competitive, does not outperform the Faster DAN in this respect, on average. Indeed, although the hyperparameters m and w can be arbitrarily chosen, the experiments showed that in practice, they must be set to a rather low value to preserve competitive recognition performance. Thus, the current state-of-the-art prediction speed for end-to-end page-level text recognition remains an issue for real-time applications. Although we limit ourselves to comparing the approaches for character-level predictions to reach state-of-the-art results with few training data, all approaches could be combined with BPE tokenization to further reduce the prediction time.

8. Conclusion

In this paper, we proposed two new prediction strategies for end-to-end full-page text recognition: windowed queries and multi-token predictions. We

show that the Meta Document Attention Network approach, combining both strategies, reaches new on-average state-of-the-art results on many handwritten datasets while reaching competitive prediction times. This approach offers a flexible balance between prediction time and recognition performance by adapting the associated hyperparameters to the given use case. While we only evaluated the Meta-DAN for HTR, the proposed approach could be applied to any autoregressive transformer-based system.

However, there is still room for improvement, and some issues remain to be solved regarding end-to-end full-page text recognition. The evaluation protocol of state-of-the-art approaches is based on training a specific model on a single dataset at a time. How to scale them to handle multilingual content, multiple reading orders (mixing Latin and Arabic languages, for instance), and highly heterogeneous layouts remains to be explored. These limited training configurations prevent the models from acquiring large, generic linguistic knowledge, leading to some failure cases when the visual content is degraded or ambiguous. Another point is about the prediction time, which remains an issue for real-time applications, as it is still in the order of magnitude of one second per document. Finally, current state-of-the-art approaches consider a single reading order per document, but this is not realistic for very complex layouts (*e.g.*, schemas, maps), for which several reading orders could be considered as humanly correct. Future works should focus on adapting metrics and losses to allow multiple reading orders for those cases.

Acknowledgment

This work was granted access to the HPC resources of IDRIS under the allocation 2024-AD011012155R2 made by GENCI. Experiments were also carried out using the Grid'5000 testbed, supported by a scientific interest group hosted by Inria and including CNRS, RENATER and several Universities as well as other organizations (see <https://www.grid5000.fr>).

References

- [1] N. Arica, F. T. Yarman-Vural, An overview of character recognition focused on off-line handwriting, *IEEE Trans. on Syst., Man, and Cybern.: Syst.* 31 (2) (2001) 216–233. [2](#)
- [2] M. A. El-Yacoubi, M. Gilloux, R. Sabourin, C. Y. Suen, An hmm-based approach for off-line unconstrained handwritten word modeling and recognition, *IEEE Trans. Pattern Anal. and Mach. Intell.* 21 (8) (1999) 752–760. [2](#)
- [3] C. Wigington, S. Stewart, B. L. Davis, B. Barrett, B. L. Price, S. Cohen, Data augmentation for recognition of handwritten words and lines using a CNN-LSTM network, in: *Int. Conf. on Doc. Anal. and Recognit.*, 2017, pp. 639–645. [2](#), [4](#)
- [4] J. Michael, R. Labahn, T. Grüning, J. Zöllner, Evaluating sequence-to-sequence models for handwritten text recognition, in: *Int. Conf. on Doc. Anal. and Recognit.*, 2019, pp. 1286–1293. [2](#), [4](#)
- [5] D. Coquenot, C. Chatelain, T. Paquet, Recurrence-free unconstrained handwritten text recognition using gated fully convolutional network, in: *Int. Conf. on Front. in Handwrit. Recognit.*, 2020, pp. 19–24. [2](#), [4](#)
- [6] T. Bluche, Joint line segmentation and transcription for end-to-end handwritten paragraph recognition, in: *Adv. in Neural Inf. Process. Syst.*, 2016, pp. 838–846. [2](#), [4](#)
- [7] T. Bluche, J. Louradour, R. O. Messina, Scan, attend and read: End-to-end handwritten paragraph recognition with MDLSTM attention, in: *Int. Conf. on Doc. Anal. and Recognit.*, 2017, pp. 1050–1055. [2](#), [4](#)
- [8] M. Yousef, T. E. Bishop, Origaminet: Weakly-supervised, segmentation-free, one-step, full page text recognition by learning to unfold, in: *Conf. on Comput. Vis. and Pattern Recognit.*, 2020, pp. 14698–14707. [2](#), [4](#)

- [9] D. Coquenot, C. Chatelain, T. Paquet, End-to-end handwritten paragraph text recognition using a vertical attention network, *IEEE Trans. on Pattern Anal. and Mach. Intell.* 45 (2023) 508–524. [2](#), [4](#), [7](#), [26](#), [37](#), [38](#)
- [10] D. Coquenot, C. Chatelain, T. Paquet, Dan: a segmentation-free document attention network for handwritten document recognition, *IEEE Trans. on Pattern Anal. and Mach. Intell.* 45 (7) (2023) 8227–8243. [2](#), [4](#), [6](#), [11](#), [14](#), [16](#), [18](#), [26](#), [38](#)
- [11] D. Coquenot, C. Chatelain, T. Paquet, Faster dan: Multi-target queries with document positional encoding for end-to-end handwritten document recognition, in: *Int. Conf. on Doc. Anal. and Recognit.*, Vol. 14190, 2023, pp. 182–199. [2](#), [4](#), [5](#), [9](#), [11](#), [14](#), [26](#)
- [12] D. Castro, B. L. D. Bezerra, C. Zanchettin, An end-to-end approach for handwriting recognition: From handwritten text lines to complete pages, in: *IEEE Conf. on Comput. Vis. and Pattern Recognit. Workshops*, 2024, pp. 264–273. [2](#)
- [13] T. Constum, P. Tranouez, T. Paquet, DANIEL: A fast Document Attention Network for Information Extraction and Labelling of handwritten documents, *Int. J. on Doc. Anal. and Recognit.* (2025). [2](#), [4](#), [5](#), [17](#), [26](#)
- [14] T. Constum, L. Preel, T. Larcher, T. Paquet, P. Tranouez, S. Bree, End-to-end information extraction in handwritten documents: Understanding paris marriage records from 1880 to 1940, in: *Int. Conf. on Doc. Anal. and Recognit.*, 2024, pp. 195–214. [2](#)
- [15] M. Boillet, S. Tarride, Y. Schneider, B. Abadie, L. Kesztenbaum, C. Kermorvant, The socface project: Large-scale collection, processing, and analysis of a century of french censuses, in: *Int. Conf. on Doc. Anal. and Recognit.*, 2024, pp. 57–73. [2](#)
- [16] S. Tarride, M. Boillet, J. Moufflet, C. Kermorvant, SIMARA: A database for key-value information extraction from full-page handwritten documents,

- in: *Int. Conf. on Doc. Anal. and Recognit.*, Vol. 14189, 2023, pp. 421–437. [2](#)
- [17] S. Tarride, M. Boillet, C. Kermorvant, Key-value inf. extraction from full handwritten pages, in: *Int. Conf. on Doc. Anal. and Recognit.*, Vol. 14188, 2023, pp. 185–204. [2](#), [26](#)
- [18] F. Gloeckle, B. Y. Idrissi, B. Rozière, D. Lopez-Paz, G. Synnaeve, Better & faster large language models via multi-token prediction, in: *Int. Conf. on Mach. Learn.*, 2024. [3](#), [5](#), [10](#)
- [19] A. Graves, S. Fernández, F. J. Gomez, J. Schmidhuber, Connectionist temporal classification: labelling unsegmented sequence data with recurrent neural networks, in: *Mach. Learn., Proc. of the Twenty-Third Int. Conf.*, Vol. 148, 2006, pp. 369–376. [4](#)
- [20] A. Graves, J. Schmidhuber, Offline handwriting recognition with multidimensional recurrent neural networks, in: *Adv. in Neural Inf. Process. Syst.*, 2008, pp. 545–552. [4](#)
- [21] M. Carbonell, A. Fornés, M. Villegas, J. Lladós, A neural model for text localization, transcription and named entity recognition in full pages, *Pattern Recognit. Lett.* 136 (2020) 219–227. [4](#)
- [22] D. Coquenat, C. Chatelain, T. Paquet, Span: a simple predict & align network for handwritten paragraph recognition, in: *Int. Conf. on Doc. Anal. and Recognit.*, Vol. 12823, 2021, pp. 70–84. [4](#)
- [23] A. Vaswani, N. Shazeer, N. Parmar, J. Uszkoreit, L. Jones, A. N. Gomez, L. Kaiser, I. Polosukhin, Attention is all you need, in: *Adv. in Neural Inf. Process. Syst.*, 2017, pp. 5998–6008. [4](#), [8](#)
- [24] K. Barrere, Y. Soullard, A. Lemaitre, B. Couïasnon, A light transformer-based architecture for handwritten text recognition, in: *Doc. Anal. Syst.*, Vol. 13237, 2022, pp. 275–290. [4](#)

- [25] S. S. Singh, S. Karayev, Full page handwriting recognition via image to sequence extraction, in: 16th Int. Conf. on Doc. Anal. and Recognit., Vol. 12823, 2021, pp. 55–69. [4](#), [7](#)
- [26] M. Schall, M. Schambach, M. O. Franz, Multi-dimensional connectionist classification: Reading text in one step, in: Int. Workshop on Doc. Anal. Syst., 2018, pp. 405–410. [4](#)
- [27] W. Qi, Y. Yan, Y. Gong, D. Liu, N. Duan, J. Chen, R. Zhang, M. Zhou, Prophetnet: Predicting future n-gram for sequence-to-sequence pre-training, in: Find. of the Assoc. for Comput. Linguist.: EMNLP, Vol. EMNLP 2020, 2020, pp. 2401–2410. [5](#)
- [28] M. Stern, N. Shazeer, J. Uszkoreit, Blockwise parallel decoding for deep autoregressive models, in: Adv. in Neural Inf. Process. Syst., 2018, pp. 10107–10116. [5](#)
- [29] Z. Fei, Partially non-autoregressive image captioning, in: Thirty-Third Conf. on Innov. Appl. of Artif. Intell., 2021, pp. 1309–1316. [5](#)
- [30] R. Sennrich, B. Haddow, A. Birch, Neural machine translation of rare words with subword units, in: Proc. of the 54th Annu. Meeting of the Assoc. for Comput. Linguist., 2016, pp. 1715–1725. [5](#)
- [31] R. J. Williams, D. Zipser, A learning algorithm for continually running fully recurrent neural networks, *Neural Comput.* 1 (2) (1989) 270–280. [15](#)
- [32] U. Marti, H. Bunke, The iam-database: an english sentence database for offline handwriting recognition, *Int. J. on Doc. Anal. and Recognit.* 5 (1) (2002) 39–46. [15](#), [16](#)
- [33] J. Sánchez, V. Romero, A. H. Toselli, E. Vidal, ICFHR2016 competition on handwritten text recognition on the READ dataset, in: Int. Conf. on Front. in Handwrit. Recognit., 2016, pp. 630–635. [15](#), [16](#)

- [34] V. Romero, A. Fornés, N. Serrano, J. Sánchez, A. H. Toselli, V. Frinken, E. Vidal, J. Lladós, The ESPOSALLES database: An ancient marriage license corpus for off-line handwriting recognition, *Pattern Recognit.* 46 (6) (2013) 1658–1669. [15](#), [16](#)
- [35] A. F. de Sousa Neto, B. L. D. Bezerra, S. S. Araújo, W. M. A. S. Souza, K. F. Alves, M. F. Oliveira, S. V. S. Lins, H. J. F. Hazin, P. H. V. Rocha, A. H. Toselli, ICDAR 2024 competition on handwritten text recognition in brazilian essays - BRESSAY, in: *Int. Conf. on Doc. Anal. and Recognit.*, Vol. 14809, 2024, pp. 345–362. [15](#), [16](#), [26](#)
- [36] H. J. G. A. Dolfing, J. R. Bellegarda, J. Chorowski, R. Marxer, A. Laurent, The "scribblelens" dutch historical handwriting corpus, in: *Int. Conf. on Front. in Handwrit. Recognit.*, 2020, pp. 67–72. [15](#), [16](#)
- [37] L. T. Tsochatzidis, S. Symeonidis, A. Papazoglou, I. Pratikakis, HTR for greek historical handwritten documents, *J. of Imaging* 7 (12) (2021) 260. [15](#), [16](#), [26](#)
- [38] C. Liu, F. Yin, D. Wang, Q. Wang, CASIA online and offline chinese handwriting databases, in: *Int. Conf. on Doc. Anal. and Recognit.*, 2011, pp. 37–41. [15](#), [16](#)
- [39] S. Brunessaux, P. Giroux, B. Grilhères, M. Manta, M. Bodin, K. Choukri, O. Galibert, J. Kahn, The maurdor project: Improving automatic processing of digital documents, in: *Int. Workshop on Doc. Anal. Syst.*, 2014, pp. 349–354. [15](#), [16](#)
- [40] E. Grosicki, M. Carré, J. Brodin, E. Geoffrois, Results of the RIMES evaluation campaign for handwritten mail process., in: *Int. Conf. on Doc. Anal. and Recognit.*, 2009, pp. 941–945. [15](#), [16](#)
- [41] E. Grosicki, M. Carré, E. Geoffrois, E. Augustin, F. Preteux, R. Messina, Rimes, complete (Mar. 2024). [doi:10.5281/zenodo.10812725](https://doi.org/10.5281/zenodo.10812725). [15](#), [16](#)

- [42] E. Grosicki, H. E. Abed, ICDAR 2011 - french handwriting recognition competition, in: *Int. Conf. on Doc. Anal. and Recognit.*, 2011, pp. 1459–1463. [16](#)
- [43] V. Lcvenshtein, Binary coors capable or ‘correcting deletions, insertions, and reversals, in: *Soviet physics-doklady*, Vol. 10, 1966. [17](#)
- [44] G. Yao, N. Ding, T. Zhao, K. Zhao, P. Tang, Y. Tao, L. Peng, Visual prompt learning for chinese handwriting recognition, in: *Int. Conf. on Doc. Anal. and Recognit.*, Vol. 14804, 2024, pp. 119–133. [26](#)
- [45] Z. Wang, Y. Yu, Y. Wang, H. Long, F. Wang, Robust end-to-end offline chinese handwriting text page spotter with text kernel, in: *Int. Conf. on Doc. Anal. and Recognit. Workshops*, Vol. 12917, 2021, pp. 21–35. [26](#)
- [46] D. H. Diaz, S. Qin, R. R. Ingle, Y. Fujii, A. Bissacco, Rethinking text line recognition models, *arXiv preprint 2104.07787* (2021). [26](#)
- [47] H. J. G. A. Dolfing, Whole page recognition of historical handwriting, *arXiv preprint 2009.10634* (2020). [26](#)
- [48] F. Chollet, Xception: Deep learning with depthwise separable convolutions, in: *IEEE Conf. on Comput. Vis. and Pattern Recognit.*, 2017, pp. 1800–1807. [37](#)

Appendix A. Datasets

Example images

Figure A.7 provides document image examples from the 10 evaluated datasets. As one can note, these datasets cover many page layouts, visual aspects, writing styles, periods, and languages.

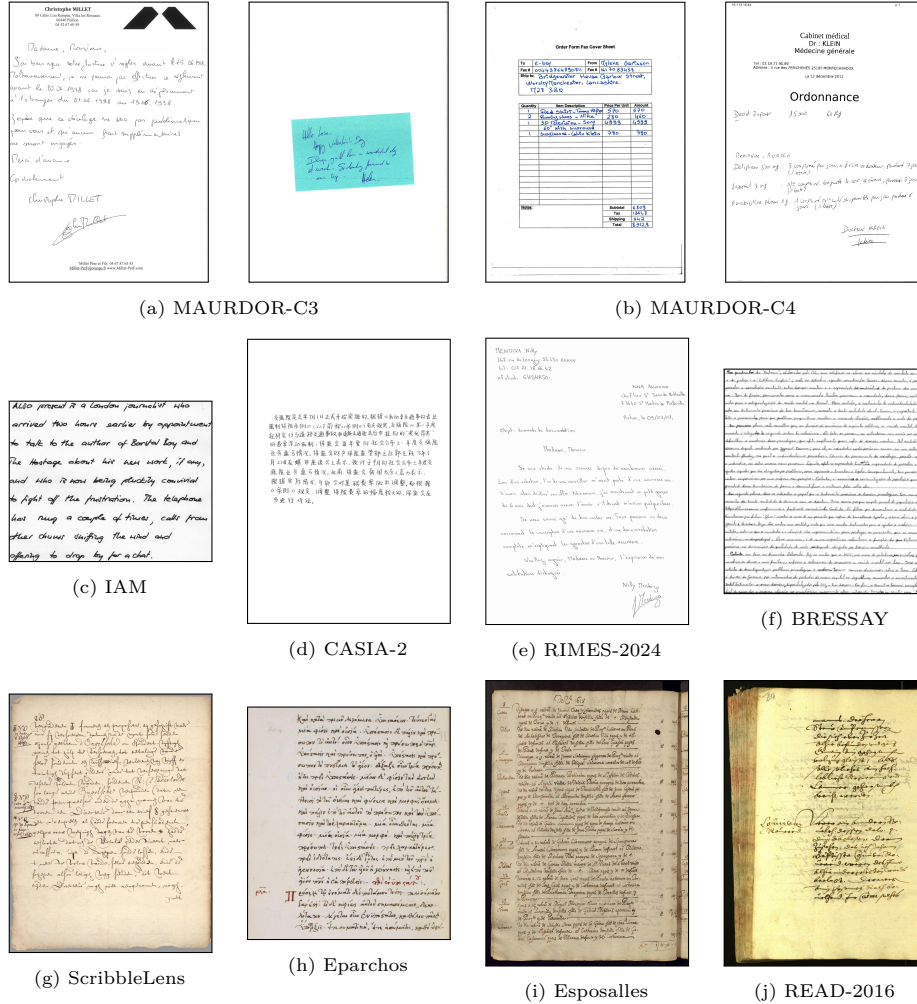


Figure A.7: Dataset samples from test sets. The MAURDOR-C3 and MAURDOR-C4 datasets provide widely heterogeneous documents in terms of layout, while the other datasets are quite homogeneous.

Line-level splits

Table A.8 details the splits for training, validation, and test used for the different datasets regarding the experiments at line level.

Table A.8: Datasets splits at line level.

Dataset	Train	Validation	Test
IAM	6,482	976	2,915
READ-2016	8,367	1,043	1,140
Esposalles	2,328	742	757
ScribbleLens	4,408	375	563
CASIA-2	36,305	5,465	10,449
Eparchos	1,512	380	380
BRESSAY	19,561	4,608	5,915

Appendix B. Scaling up the DAN encoder

We noticed that the DAN lacked some feature extraction capability when evaluated on challenging datasets such as BRESSAY, which presents some crossed-out text with annotations. We opt for scaling up the DAN encoder only in order to increase the performance while preventing a significant prediction time increase. Indeed, the encoding part of the model is only used once at inference (it is excluded from the iterative decoding stage); so the computations involved are not such significant compared to decoding. The proposed encoder is referred to as FCN-M, and the original one as FCN-S.

The proposed modification mainly consists in doubling the number of feature maps per block while preserving the last one, which conditions the size of the decoder, as detailed in Table B.9. We use the notation of the original paper [9], where ConvBlock is a Convolution Block made up of three convolutions, instance normalization, and dropout. DSCBlock is equivalent except for the convolutions that are replaced by Depthwise Separable Convolutions [48].

We evaluate these modifications on READ-2016, CASIA-2, BRESSAY, and IAM datasets at line level, and at page level with the DAN. Results are shown in Table B.10. As one can note, the modified encoder improves the recognition results (or is equivalent) on all the evaluated datasets, whether it is at line or

Table B.9: Composition of the two versions of the encoder. ConvBlock(X) and DSCBlock(X) indicate the number of feature maps X returned by each convolutional layer.

	FCN-S [9]	FCN-M (ours)	Output size
layers	ConvBlock(16)	ConvBlock(32)	$H \times W$
	ConvBlock(32)	ConvBlock(64)	$\frac{H}{2} \times \frac{W}{2}$
	ConvBlock(64)	ConvBlock(128)	$\frac{H}{4} \times \frac{W}{4}$
	ConvBlock(128)	ConvBlock(256)	$\frac{H}{8} \times \frac{W}{8}$
	ConvBlock(128)	ConvBlock(512)	$\frac{H}{16} \times \frac{W}{8}$
	ConvBlock(128)	ConvBlock(512)	$\frac{H}{32} \times \frac{W}{8}$
	DSCBlock(128)	DSCBlock(512)	$\frac{H}{32} \times \frac{W}{8}$
	DSCBlock(128)	DSCBlock(512)	$\frac{H}{32} \times \frac{W}{8}$
	DSCBlock(128)	DSCBlock(512)	$\frac{H}{32} \times \frac{W}{8}$
	DSCBlock(256)	DSCBlock(256)	$\frac{H}{32} \times \frac{W}{8}$
# params	1.7 M	17.6 M	

Table B.10: Impact of the encoder changes at line (pre-training stage) and page levels. CER are expressed in percentages, and times in seconds.

Dataset	Encoder	FCN (line)		DAN (page)	
		CER	Time	CER	Time
READ-2016	FCN-S	4.82	0.03	3.82	4.61
	FCN-M	4.61	0.03	<u>3.85</u>	4.88
CASIA-2	FCN-S	5.33	0.05	1.35	2.94
	FCN-M	2.91	0.05	1.10	2.81
Bressay	FCN-S	6.11	0.02	4.53	24.28
	FCN-M	3.45	0.02	2.43	24.65
IAM	FCN-S	5.76	0.03	4.53	3.57
	FCN-M	4.84	0.03	4.23	3.39

page level. The prediction time is only slightly impacted; we assume this is mainly due to the complexity of learning the reading order. For CASIA-2 and IAM, the prediction time is lower, which can be explained by a reduction of the loop effect (predicting several times the same text part). But for READ-2016 and BRESSAY, the prediction time is higher, which can be the result of the additional computations due to the bigger encoder, and to better recognition (missed text parts are now well recognized, adding extra decoding iterations). The most negative impact is on the READ-2016 dataset with a 6% increase in the prediction time. These results also enhance what has been found in [10]: the page-level DAN outperforms its line-level counterpart while they are based on the same encoder.

Appendix C. WER results comparing the prediction strategies.

Table C.11 provides the WER scores associated with the experiments related to Section VI-E, *i.e.*, when relying on the FCN-M encoder.

Table C.11: WER results (in percentages) on the test sets with FCN-M encoder. We used $m = 5$ and $w = 5$ for the proposed approaches. Best results at page level are shown in bold.

Dataset	Line-level	Page-level				
	FCN	DAN	Faster DAN	W-DAN	MT-DAN	Meta-DAN
IAM	15.83	14.00	13.42	16.28	14.96	15.78
BRESSAY	12.12	7.85	8.03	9.72	8.28	8.46
READ-2016	20.41	14.69	14.83	16.90	14.90	16.03
Esposalles	2.61	6.60	2.73	6.63	3.09	3.09
ScribbleLens	20.38	19.66	18.64	21.19	18.92	19.71
Eparchos	26.29	22.36	22.36	24.71	23.39	23.69
RIMES-2009	X	14.35	12.99	15.12	12.67	12.96
RIMES-2024	X	8.72	8.30	9.35	8.00	8.72
MAURDOR-C3	X	28.43	19.82	20.71	27.46	20.23
MAURDOR-C4	X	14.80	16.19	13.50	13.15	13.48
Average	X	15.15	13.73	15.41	14.48	14.22

Interestingly, the WER results do not follow exactly the same trend as that of the CER, by exhibiting a slight advantage for the Faster DAN, which reaches an on-average WER of 13.73%, compared to 14.22% for the Meta-DAN. There is no clear explanation for this observation. However, it still remains lower than the DAN WER, which reaches 15.15%. This would suggest that the Faster-DAN is more reliable when its initial predictions are correct, leading to perfectly recognized words (lower WER), but that bad starts cause cascading errors, leading to higher CER, while the proposed Meta-DAN is more constant in character recognition performance.